Synthesis and Associating Properties of Poly(ethoxyethyl glycidyl ether)/Poly(propylene oxide) Triblock Copolymers

Philip Dimitrov,[†] Stanislav Rangelov,[†,‡] Andrzej Dworak,[§] and Christo B. Tsvetanov*[,†]

Institute of Polymers, Bulgarian Academy of Sciences, 1113 Sofia, Bulgaria, Institute of Coal Chemistry, Polish Academy of Sciences, 44-102 Gliwice, Poland, and Department of Physical Chemistry, University of Uppsala, 751 23 Uppsala, Sweden

Received September 19, 2003; Revised Manuscript Received November 7, 2003

ABSTRACT: A number of ABA and BAB triblock copolymers of ethoxyethyl glycidyl ether (EEGE) and propylene oxide (PO) were prepared by sequential anionic polymerization. The copolymers were characterized by nuclear magnetic resonance and gel permeation chromatography. The total number-average molecular weights were in the range 1000−9000, whereas the degrees of polymerization of the PPO and PEEGE blocks varied from 2 to 34 and from 3 to 17, respectively. The copolymers were comprised of blocks with different lower critical solution temperatures (LCSTs) in aqueous media. Their self-association in aqueous environment was studied by cloud point (CP) measurements, dye solubilization, light scattering, ^{1}H nuclear magnetic resonance, and scanning electron microscopy. Although the behavior of the copolymers was found to depend on their architecture, the PO/EEGE ratio, and the degrees of polymerization of the different blocks, the role of the PEEGE blocks was decisive: it is PEEGE that determines the LCST properties of the copolymers as well as their CP and critical micelle concentration values. The copolymers form nanosized particles as revealed by light scattering. The aggregates exhibit different temperature behavior depending on the copolymer architecture. The aggregates of the copolymers of a normal, i.e., ABA, architecture were found to undergo a secondary aggregation at certain temperatures, whereas those of the BAB copolymers gradually increased in size with increasing temperature. The difference is attributed to the different arrangement of the chains in the corona regions, directly affecting the continuity and thickness of the corona.

Introduction

Self-association of amphiphilic block copolymers in selective solvents can result in the formation of various structures with dimensions ranging from nano- to microscopic. It has been shown that ABA block copolymers, where A stands for the hydrophilic block and B for the hydrophobic block, are able to undergo core−shell micelle formation in aqueous solution.[1−7] The self-assembly of copolymers of a reverse, i.e., BAB architecture usually results in the formation of more complex structures, such as flowerlike and linked micelles and networks.[8−13]

The preparation of nanoscale polymeric micelles from amphiphilic block copolymers involves precise adjusting of the hydrophilic−hydrophobic balance of the system.[14−18] Thus, by altering the ratio between the hydrophilic and the hydrophobic monomeric units, as well as the length of the hydrophobic blocks, one can effectively control the morphology and the size of the aggregates. In the majority of cases the hydrophilic block is poly(ethylene oxide) (PEO), which is soluble in water within the whole temperature interval from 0 to 100 °C. The hydrophobic block is represented by a much wider range of polymers. Generally, they can be divided into two basic groups: (1) truly hydrophobic polymers—such as polystyrene, polybutadiene, etc.; (2) stimuli-responsive polymers—water-soluble at given conditions, but after a change in the environmental conditions they become insoluble. The latter class includes an interesting type of polymers that exhibit lower critical solution temperature (LCST) properties in aqueous media. Recently, they have attracted great attention, due to their unique ability to undergo a temperature-induced phase separation from the soluble state to the insoluble state. If such a type of polymer serves as a B block, a mere increase of the temperature induces self-association.[19−23] A typical example is the oligomeric poly(propylene oxide) (PPO),[24−26] which builds the hydrophobic block in the most extensively studied polymeric nonionic surfactants, PEO/PPO/PEO, commercially available as Pluronics (BASF) or Synperonics (ICI).

It is known, however, that PEO/PPO/PEO micelles are not stable at low temperatures; they disintegrate, which leads to reduction and even loss of their efficiency as surfactants. Having this in mind, our attention was focused on such triblock copolymers that would form stable aggregates in water even at temperatures close to 0 °C. This would benefit technological processes that require such temperature regimes. We have recently found that oligomeric poly(ethoxyethyl glycidyl ether) (PEEGE) of $M_n = 2000$ is water-soluble below 11 °C; i.e., it exhibits LCST properties. On the other hand PPO 2000 has an LCST close to 19 °C,[25] and therefore, PEEGE is considered to be more hydrophobic than PPO of corresponding molecular weight. PEEGE was synthesized by anionic polymerization of EEGE using various initiators as reported elsewhere.[27] Dworak et al. obtained triblock copolymers of EEGE and ethylene oxide via the poly(ethylene glycol) macroinitiator technique.[28] Our aim was to prepare triblock copolymers comprising PEEGE and PPO blocks, thus obtaining copolymers built of thermosensitive blocks, which might

* To whom correspondence should be addressed. Fax: (+359 2) 8707523. E-mail: chtsvet@polymer.bas.bg.
† Bulgarian Academy of Sciences.
‡ University of Uppsala.
§ Polish Academy of Sciences.

10.1021/ma0354039 CCC: $27.50
Published on Web 01/09/2004

possess potentially interesting associating properties in aqueous solution.

In the present work ABA and BAB triblock copolymers of PO and EEGE were synthesized via sequential anionic polymerization using cesium alkoxide initiators. Their self-association in aqueous media was studied by cloud point measurements, the dye solubilization technique, light scattering (LS), ^{1}H nuclear magnetic resonance, and scanning electron microscopy.

Experimental Section

A. Materials. All solvents were purified by standard methods. PO (Aldrich) was freshly distilled over CaH_2 before use. PPO 2000, purchased from Aldrich, was used without further purification. EEGE was obtained by a procedure described elsewhere.[29] It was distilled under vacuum, and fractions with purity exceeding 99.0% determined by gas chromatography were used for polymerizations. Cesium hydroxide monohydrate (99.5%, Acros Organics) was used as received. 1,2-Propanediol was purified by vacuum distillation.

B. Synthesis of Block Copolymers. 1. Polymerization Initiated by Cesium Alkoxide of 1,2-Propanediol. To 2 mmol of cesium hydroxide monohydrate magnetically stirred in a reaction vessel equipped with argon and vacuum lines was added 1 mmol of 1,2-propanediol diluted in THF at 90 °C. After 2 h of stirring, 1 mL of dry benzene was added and the system was switched to the vacuum line (1×10^{-3} bar) for another 2 h in order to remove released water. An appropriate quantity of monomer (PO or EEGE) was introduced to the initiator at 60 °C. The polymerization leading to formation of the central block was completed in 24 h. After removal of a sample for analysis an appropriate quantity of the other monomer was added. The polymerization was terminated after 48 h by adding methanol.

PEEGE homopolymers were synthesized similarly.

2. Polymerization Initiated by Poly(propylene glycol) Macroinitiator. To 1.5 mmol of PPO 2000 magnetically stirred in a reaction vessel equipped with argon and vacuum lines was added 3.3 mmol of cesium hydroxide monohydrate at 90 °C. After 2 h 1 mL of dry benzene was added, and then the vacuum line was switched on for 2 h. Then an appropriate amount of EEGE monomer was introduced to the obtained macroinitiator at 60 °C. The polymerization of EEGE was terminated after 48 h by adding methanol.

3. Purification of Copolymers. The copolymer viscous liquid was filtered from the insoluble precipitate of MeOCs formed during the termination. Afterward the residue was dissolved in distilled water at 0 °C and extracted with $CHCl_3$. After evacuation of the solvent the residue was dissolved in benzene and freeze-dried.

C. Methods. 1. NMR. The ^{1}H and ^{13}C NMR spectra were recorded at 250 and 62.5 MHz, respectively, on a Bruker WM 250, using $CDCl_3$ or D_2O as solvent.

2. Size Exclusion Chromatography (SEC). Measurements were performed on a Waters system consisting of four Styragel columns with nominal pore sizes of 100, 500, 500, and 1000 Å, eluted with THF at 40 °C. The eluent flow rate was 1 mL·min^{-1}. Toluene was used as the internal standard for indication of elution volumes. Calibration was made with polystyrene standards.

3. Cloud Point Measurements. Cloud point (CP) transitions of 2% aqueous solutions of the samples were followed on a Specord UV−vis spectrometer (Carl Zeiss, Jena, Germany) switched to the transmittance regime at $\lambda = 500$ nm using a thermostated cuvette holder. The solutions were equilibrated for 12 h at 0 °C and then heated slowly (0.2 °C min^{-1}).

4. Determination of the Critical Micellization Concentration (cmc). Aqueous solutions (2 mL) of a triblock copolymer in the concentration range from 0.2 to 20 g/L were prepared at 0 °C. A 20 μL sample of a 0.4 mM solution of 1,6-diphenyl-1,3,5-hexatriene (DPH) in methanol was added to each of the copolymer solutions. The solutions were incubated in the dark for 16 h at 20 °C. The absorbance in the range of $\lambda = 300-500$ nm was followed at 20 and 30 °C on a Specord UV−vis spectrometer. The main absorption peak characteristic of DPH solubilized in a hydrophobic domain was observed at 356 nm.[30]

5. Light Scattering Measurements. The light scattering setup has been described previously.[31] It consists of a 488 nm Ar ion laser and detector optics with an ITT FW 130 photomultiplier and ALV-PM-PD amplifier discriminator connected to an ALV-5000 autocorrelator built into a computer. The cylindrical scattering cells were sealed and then immersed in a large-diameter thermostated bath containing the index matching fluid decalin. Measurements were made at different angles in the range of 50−130° and at different temperatures. Information about the radii of gyration, R_g, was obtained from the dependence of the quantity $1/(I \sin\theta)$, which is proportional to the reduced scattered intensity, on the scattering angle, θ. R_g was determined from the ratio of the initial slope to the intercept of such plots.

Analysis of the dynamic data was performed by fitting the experimentally measured $g_2(t)$, the normalized intensity autocorrelation function, which is related to the electrical field correlation function $g_1(t)$ by the Siegert relationship:[32]

$$g_2(t) - 1 = \beta|g_1(t)|^2 \tag{1}$$

where β is a factor accounting for deviation from ideal correlation. For polydisperse samples, $g_1(t)$ can be written as the inverse Laplace transform (ILT) of the relaxation time distribution, $\tau A(\tau)$:

$$g_1(t) = \tau \mathrm{A}(\tau) \exp(-t/\tau)\, \mathrm{d} \ln \tau \tag{2}$$

where τ is the lag time. The relaxation time distribution, $\tau A(\tau)$, was obtained by performing ILT using the constrained regularization algorithm REPES, which minimizes the sum of the squared differences between the experimental and the calculated $g_2(t)$.[33] A mean diffusion coefficient D was calculated from the second moment of each peak as $D = \Gamma/q^2$, where q is the magnitude of the scattering vector $q = (4\pi n/\lambda)\sin(\theta/2)$ and $\Gamma = 1/\tau$ is the relaxation rate of each mode. Here θ is the scattering angle, n is the refractive index of the medium, and λ is the wavelength of the light in a vacuum. The diffusion coefficients at $\theta = 90°$, D_{90}, were calculated as $D_{90} = \Gamma_{90}/q_{90}^2$, where Γ_{90} and q_{90} are the relaxation rate and scattering vector at 90°, respectively.

The hydrodynamic radii, R_h, and hydrodynamic radii at $\theta = 90°$, R_h^{90}, were calculated using the Stokes−Einstein equation:

$$R = kT/(6\pi\eta D) \tag{3}$$

Here, kT is the thermal energy factor, η is the temperature-dependent viscosity of the solvent, D is either the mean diffusion coefficient or the diffusion coefficient at $\theta = 90°$, and R is either R_h or R_h^{90}.

6. Scanning Electron Microscopy. Nanoparticles of triblock copolymers were prepared via the direct dissolution method.[15] Copolymer aqueous solutions were initially equilibrated at 0 °C and then thermostated while being magnetically stirred for 1 h at optimal temperature determined according to the cloud point value for a given sample. Samples for scanning electron microscopy were prepared by removing the solvent under vacuum followed by carbon and gold coating under vacuum. Measurements were made with a JEOL JSM-5300 apparatus.

Results and Discussion

A. Synthesis of PO/EEGE Triblock Copolymers. The anionic polymerization of PO using conventional initiators such as potassium hydroxide or potassium alkoxides is difficult to control. PO partially isomerizes to allyl alcohol in the presence of such initiators; hence, the resulting polymers possess broadened molecular

Scheme 1

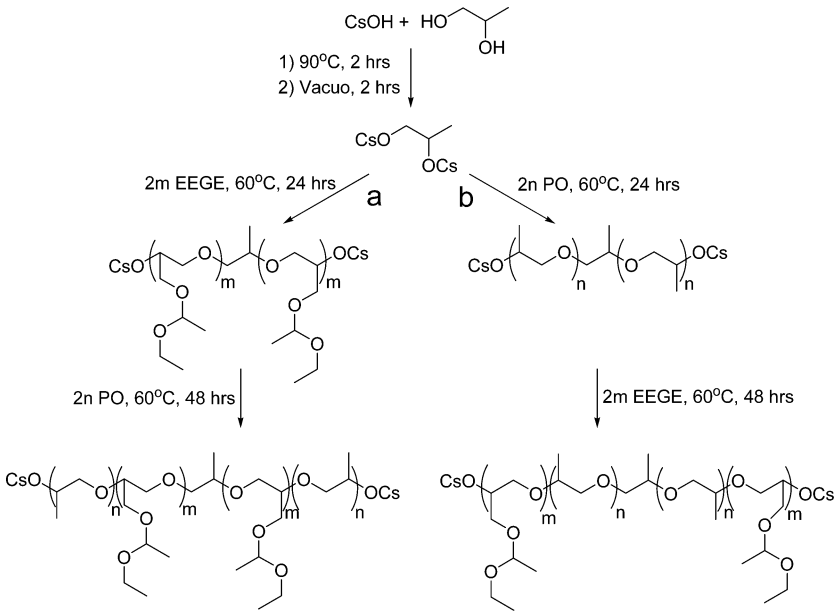

weight distributions, as well as a substantial amount of terminal double bonds.[34−36] The tendency of PO to isomerize to allyl alcohol decreases in the following order of alkali-metal counterions:[37]

$$Li^+ > Na^+ > K^+ > Rb^+ > Cs^+$$

Consequently, the above side reactions may be overcome to a great extent by using cesium initiating systems. For the synthesis of PO/EEGE block copolymers we used an initiating system similar to that described by Simons and Verbanc.[34] Instead of KOH, we employed CsOH·H_2O to diminish the PO side reactions. In addition, the cesium alkoxides are very active even at low temperatures, which is also important for the block copolymer synthesis. For better control, anhydrous conditions were kept during the polymerizations.

The anionic ring-opening polymerization of EEGE does not involve intramolecular transitions or side reactions.[27] The synthetic routes of the cesium-initiated anionic sequential block copolymerization of PO and EEGE are presented in Scheme 1. When PPO macroinitiator is used, the route described in Scheme 1b excludes the stage of PO polymerization.

B. Characterization of the Copolymers. SEC measurements of the copolymers obtained using cesium alkoxide of 1,2-propanediol as an initiator gave monomodal distributions, implying that no homopolymeric fractions of both PPO and PEEGE are formed during the copolymer synthesis (not shown). In contrast, when the macroinitiator method was used, a tiny low molecular weight tail was observed (Figure 1). Most likely this could be attributed to the presence of homo-PPO and/or diblock copolymer impurities. Obviously, PPO 2000 is not 100% bifunctional, which is often inevitable for commercial products.

The main characteristics of the copolymers are presented in Table 1. The molar ratio of the PO and the EEGE monomeric units was estimated by calculating the characteristic peak integrals from the ^{1}H NMR spectra of the copolymers (Figure 2). It should be emphasized that no signals relative to allyl end groups were detected. Thus, it was possible to calculate the number-average molecular weights of the copolymers

Table 1. Molecular Weight and Composition Characterization Data of PO/EEGE Triblock Copolymers

no.	copolymer	PO/EEGE (^{1}H NMR) (mol %/mol %)	$\bar{M}_n$ (NMR)	$\bar{M}_n$[a] (SEC)	$\bar{M}_w/\bar{M}_n$[a] (SEC)
A1	$PO_4EEGE_5PO_4$	62/38	1200	1000	1.3
A2	$PO_2EEGE_6PO_2$	40/60	1100	1200	1.2
A3	$PO_5EEGE_{16}PO_5$	38/62	2900	2200	1.3
B1	$EEGE_3PO_6EEGE_3$	50/50	1200	1000	1.3
B2	$EEGE_4PO_5EEGE_4$	38/62	1500	1300	1.3
B3	$EEGE_5PO_5EEGE_5$	33/67	1800	1500	1.3
B4	$EEGE_{10}PO_{17}EEGE_{10}$	46/54	3900	3500	1.3
B5	$EEGE_{13}PO_{34}EEGE_{13}$	57/43	5800	5500	1.2
B6	$EEGE_{15}PO_{34}EEGE_{15}$	53/47	6400	6500	1.2
B7	$EEGE_{17}PO_{34}EEGE_{17}$	50/50	7800	9000	1.2

[a] Determined using PS standards.

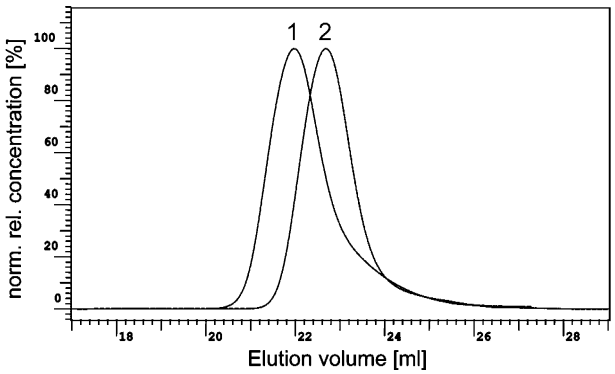

Figure 1. SEC traces of PEEGE-*block*-PPO-*block*-PEEGE (1) and initial PPO macroinitiator (2).

regarding to the integral of the *CH*OH terminal group signal at δ 3.9 ppm. Figure 3 shows a ^{13}C NMR spectrum of a PPO/PEEGE/PPO copolymer. Due to the influence of the end groups as well as of the neighboring monomeric units of the different blocks, methylene carbon atoms 2, 3, and 5 exhibit complex patterns. Similar and even more complex behavior was observed by Spassky et al. for oligo[(*R,S*)-EEGE].[27]

C. Aqueous Solution Properties of PO/EEGE Triblock Copolymers. 1. Cloud Point Measurements. Clouding temperatures of a number of PEEGE and PPO homopolymers of different molecular weights

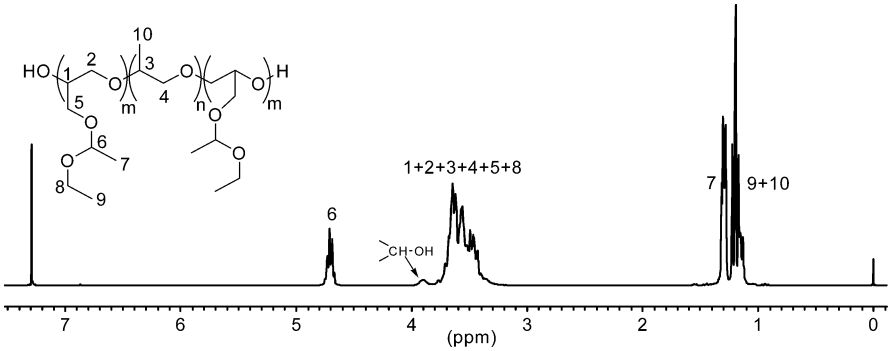

Figure 2. ^{1}H NMR spectrum of $EEGE_5PO_5EEGE_5$ (B3) in $CDCl_3$.

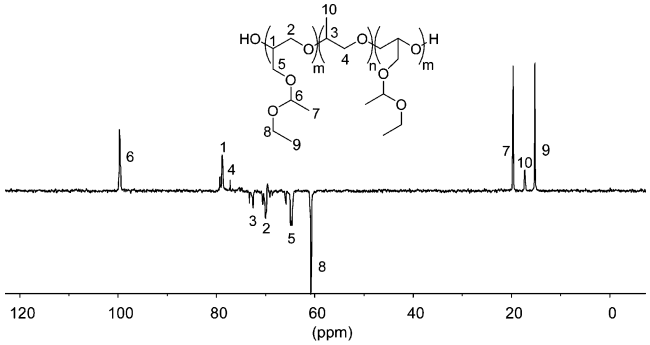

Figure 3. ^{13}C NMR spin−echo spectrum of $EEGE_5PO_5EEGE_5$ (B3) in $CDCl_3$.

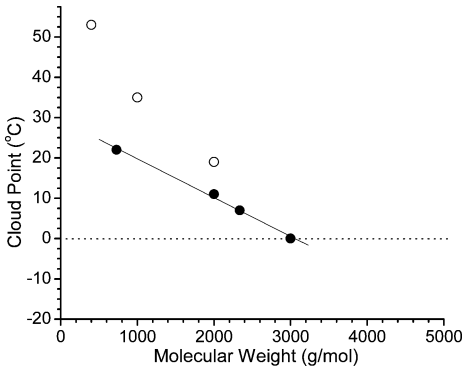

Figure 4. Influence of the molecular weight on the CP temperatures of PEEGE (filled circles) and PPO (hollow circles) aqueous solutions. c = 20 g/L.

were determined by monitoring the variations of the transmittance of 20 g/L aqueous solutions. By using the experimental and literature[24−26] data, it was possible to construct a simple phase diagram of both homopolymers (Figure 4). CPs of the homopolymers were found to decrease with increasing molecular weight. The dependence is almost linear (correlation coefficient of 0.998) for PEEGE. The curve of PEEGE is shifted to lower temperatures, which indicates that the latter is more hydrophobic than PPO.

The clouding process of the PO/EEGE copolymers is presented by a sigmoidal curve (Figure 5a), corresponding to a thermally induced phase separation that leads to a dramatic decrease of the transmittance. The process can be monitored visually due to the resulting milky-white opalescence of the solution at a given critical temperature. Clouding was observed for all of the copolymers at a given copolymer concentration (20 g/L). The presence of only one transition, which was rather sharp for all copolymers, indicates that the clouding process can be attributed mainly to the intermolecular

Table 2. Experimental and Predicted Cloud Points and cmc Data for PO/EEGE Block Copolymers[a]

no.	copolymer	CP[b] (°C)	CP_{pr}[c] I	CP_{pr}[c] II	cmc at 20 °C (g/L)	cmc at 30 °C (g/L)
A1	$PO_4EEGE_5PO_4$	19	22		3	0.75
A2	$PO_2EEGE_6PO_2$	23	21		4.9	2.6
A3	$PO_5EEGE_{16}PO_5$	7	7		0.31	0.24
B1	$EEGE_3PO_6EEGE_3$	18	25	21		
B2	$EEGE_4PO_5EEGE_4$	18	24	18	1.85	0.55
B3	$EEGE_5PO_5EEGE_5$	11	22	15	0.64	0.27
B4	$EEGE_{10}PO_{17}EEGE_{10}$	7	15	1		
B5	$EEGE_{13}PO_{34}EEGE_{13}$	8	11	−7	0.12	0.10
B6	$EEGE_{15}PO_{34}EEGE_{15}$	7	8	−13	0.06	0.05
B7	$EEGE_{17}PO_{34}EEGE_{17}$	7	5	−18	0.08	0.07

[a] See Figure 4 and the text for more information. [b] Determined at a concentration of 20 g/L. [c] Predicted CP: I, CP of a PEEGE single block; II, CP of the corresponding overall M_n of PEEGE blocks.

collapse of the more hydrophobic PEEGE blocks. This is proved by ^{1}H NMR measurements in D_2O as seen in Figure 5b. Even at 4 °C the signals of the acetal methyl protons at 1.27 and 1.33 ppm are lower than the signal of the methyl protons of the PO units. Moreover, due to poor solubilization the signals of acetal methyl protons are overlapped. As a consequence the signal at 1.27 ppm completely disappears at 15 °C. This unambiguously confirms that the aggregation process begins with dehydratation of the PEEGE blocks.

The copolymers B1 and A2 constitute a suitable pair to probe the effect of the chain architecture. Although of the same molecular weight, A2, which contains more hydrophobic EEGE units per hydrophobic block, shows a higher cloud point than B1 (Figure 5a, Table 2). Their clouding behavior is in line with the findings of other authors[10,13] reporting lower solubility of the copolymers of reverse architecture.

To follow the effect of the relatively more hydrophilic PPO block, the clouding temperatures of the copolymers were predicted and compared to the experimental data (Table 2). The predicted CP values were determined from the linear fit of the dependence CP vs molecular weight for homo-PEEGE (Figure 4) taking into account either the molecular weight of the single PEEGE block or the overall molecular weight of the two PEEGE blocks. As seen from Table 2, the PPO−PEEGE−PPO copolymers (A1, A2, and A3) clouded at temperatures close to the predicted ones. The clouding behavior of the copolymers of reverse architecture was more complex and depended very much on the length of the middle PPO block that acted as a hydrophilic spacer. Copolymers with a short PPO block (B1, B2, and B3) clouded at temperatures corresponding to a PEEGE homo-

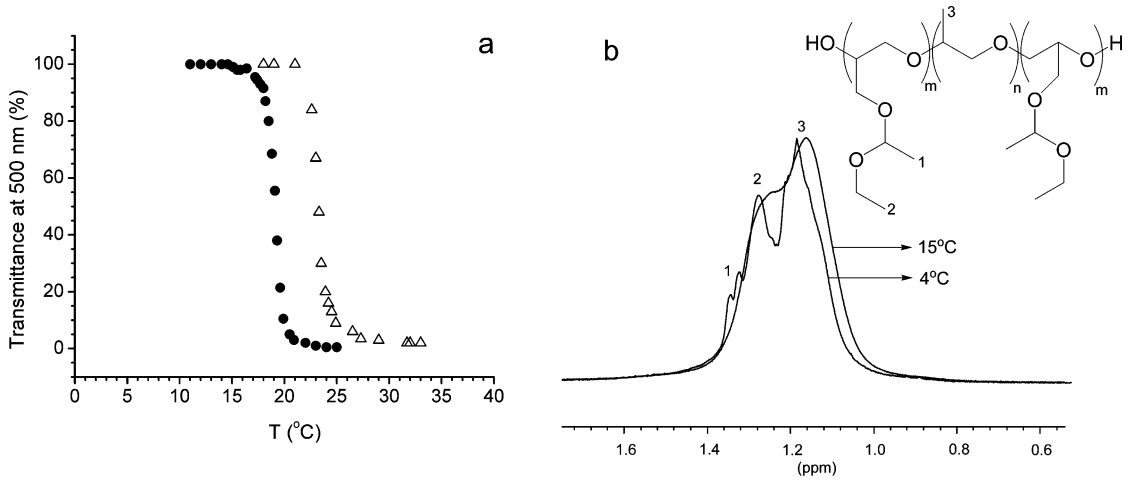

Figure 5. (a) Clouding curves of $EEGE_3PO_6EEGE_3$ (B1) (circles) and $PO_2EEGE_6PO_2$ (A2) (triangles). $c = 20$ g/L. (b) ^{1}H NMR in D_2O of $EEGE_{10}PO_{17}EEGE_{10}$ at 4 and 15 °C.

polymer of the same molecular weight as the overall molecular weight of the side PEEGE blocks. Apparently, the length of the PPO block was insufficient to provide independent behavior of the PEEGE blocks. In contrast, copolymers with a much longer PPO spacer (B5, B6, and B7; $DP_{PPO} = 34$) cloud at temperatures very close to that of a PEEGE homopolymer of molecular weight equal to that of a single PEEGE block within the macromolecule. Obviously, in this case the length of the PPO block turned out to be critical. In conformity with these observations an experimental CP value of 7 °C was observed for the copolymer with an intermediate degree of polymerization of the middle PPO block, B4. This value lies exactly between the predicted values for the single PEEGE block and the overall PEEGE molecular weight (Table 2). Presumably the hydrophilicity of PPO also has an effect on phase separation. The interplay of length and hydrophilicity is probably reflected from the behavior of the copolymer with an intermediate PPO length, B4. However, limitations of sample availability prevented us from elucidating the effect of hydrophilicity.

2. Critical Micellization Concentration Data. The solubilization of 1,6-diphenyl-1,3,5-hexatriene in PEO/PPO/PEO aqueous solutions for spectroscopic determination of the critical micellization concentration was introduced by Alexandridis et al.[30] and was successfully utilized by other authors for characterization of various amphiphilic block copolymer systems.[38−40] The main difference in our system was that the PPO blocks here play the role of a relatively more hydrophilic part of the macromolecule. The cmc's were determined from the first inflection of DPH absorption intensity as shown in Figure 6 and collected in Table 2. The length of hydrophobic PEEGE blocks greatly affected the micellization process: the higher the DP of PEEGE blocks, the lower the cmc at a given temperature. As shown in Figure 6 the increase of the temperature led to a significant change of the cmc value of PO/PEEGE copolymers with shorter PEEGE blocks, which is typical for common amphiphilic block copolymers.[30,41] The temperature effect weakened with the increase of the DP of PEEGE blocks. A noticeable effect on the copolymer architecture was not observed.

3. Light Scattering Measurements. To obtain additional information on the hydrodynamic behavior of the copolymers, static and dynamic light scattering

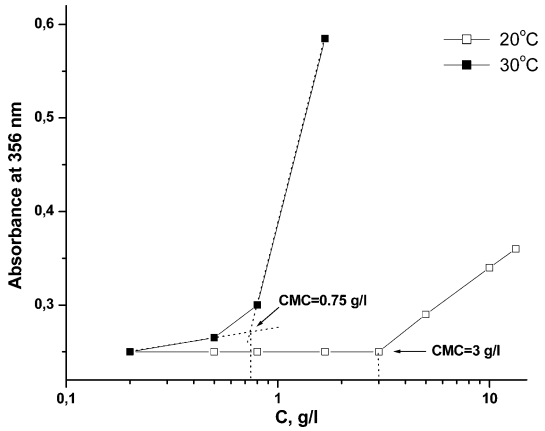

Figure 6. Variation of the absorbance of DPH at 356 nm with $PO_4EEGE_5PO_4$ (A1) concentration at two temperatures.

were carried out simultaneously within an extended temperature range. The measurements were performed at single concentrations which were always higher than the cmc's determined from the dye-solubilization method.

3.1. PPO/PEEGE/PPO Architecture. Examples of relaxation time distributions for the copolymers with the lowest (A1) and the highest (A3) EEGE content are shown in Figure 7. The distributions in the investigated temperature intervals are predominantly bimodal. The peaks are diffusive as demonstrated in Figure 8 for both modes of A3 at 5 °C. Their amplitudes vary within the sample composition and the temperature. As seen in Figure 7 at the lowest EEGE content (sample A1) the particles responsible for the fast mode contribute about 30% of the total scattered light intensity at 7 °C, whereas the corresponding value for A3 is less than 2%.

Upon heating, the fast mode amplitudes decrease progressively and completely disappear at 23 and 11.5 °C for A2 and A3, respectively. In contrast, a fast mode is still detectable at temperatures as high as 50 °C for A1. The fast modes correspond to particles with hydrodynamic radii, R_h, of about 5.7, 9.3, and 12.4 Å for A1, A2, and A3, respectively. These experimental values are consistent with the values obtained using the power law between R_h and molecular weight given by the empirical relationship (eq 4) established for a polymer in good solvent systems.[42] It is conceivable, therefore, to assume that a fraction of unassociated molecules, unimers,

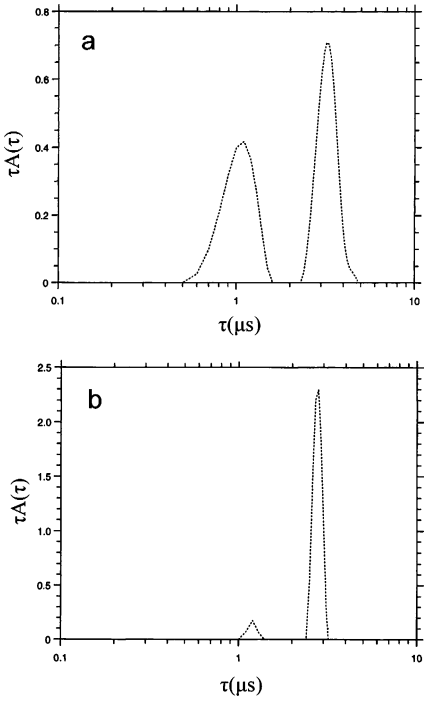

Figure 7. Relaxation time distributions measured at an angle of 90° of (a) A1 at 4.4 g/L and 7 °C and (b) A3 at 3.2 g/L and 5 °C.

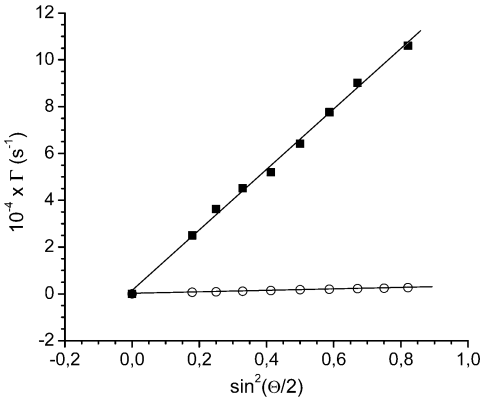

Figure 8. Relaxation rate (Γ) of the fast (squares) and dominant (circles) modes as a function of $\sin^2(\theta/2)$ for A3 at 3.2 g/L and 5 °C. The lines through the data represent linear fits to the data.

exists. It decreases progressively upon heating, indicating that unimers are incorporated into the aggregates.

$$R_h = 0.116 M_w^{0.566} \text{ (Å)} \quad (4)$$

Figure 9a shows the variations of the scattered light intensity at $\theta = 90°$ with temperature. The effect of the PEEGE block size is clearly seen. Although I_{90} slightly increases at $T > 30$ °C, the I_{90} readings for A1 are generally low in the whole temperature interval. A2 exhibits a similar curve pattern with three distinguishable differences compared to A1: (i) I_{90} is invariably larger; (ii) its increase is considerably sharper (note the logarithmic scale of I_{90}) and (iii) is shifted toward lower temperatures. Perhaps, the curve pattern for A3 is the same, implying that a low-temperature interval, in which the I_{90} readings are low and change only slightly with temperature, exists. However, this temperature interval is very narrow and not accessible in our measurements. It is also seen that I_{90} for A2 and A3 reaches a maximum at certain temperatures and then drops. Since at these temperatures the dispersions become milky-white opalescent, this feature can be attributed to multiple scattering.[43,44] The temperatures at which the milky-white opalescence appears are consistent with the CP measurements. The slight difference can be attributed to the different concentration ranges studied in the CP and LS measurements. There is, however, discrepancy between the CP and LS data of A1 dispersions. As shown above, A1 behaves differently from A2 and A3: it is less able to self-associate as revealed by the presence of fast modes of high amplitudes, and on the other hand the aggregates that are formed are somewhat larger than those of A2 and A3 (Figure 9b). Presumably the aggregates are formed by copolymer molecules of high EEGE content (note the relatively high polydispersity index). At high concentrations they cause clouding at much lower temperatures than expected for a copolymer with a composition like that of A1.

Figure 9b shows the variations of the radii of the particles responsible for the dominant mode with the temperature. In the low-temperature regions, where the dimensions of the particle do not change, the particles are presumably of core/corona architecture with cores consisting mainly of PEEGE moieties and coronae built of PPO. The width of these regions depends on the copolymer composition and is found to decrease with increasing EEGE content. With increasing temperature, PPO progressively becomes dehydrated, which most probably affects the continuity and thickness of the protective shell. At certain temperatures, which are obviously composition-dependent, the PPO blocks are no longer able to stabilize the aggregates and secondary aggregation takes place. This is clearly demonstrated in Figure 9b for the copolymers A1 and A2, whereas the dependence of A3 is somewhat peculiar. As mentioned above the low-temperature region in which we can expect temperature independence of the particle size is not accessible. Most probably, the curve pattern reflects changes in the dimensions after the secondary aggregation has taken place. The break in the dependence indicates that the latter proceeds with different rate constants, which can be attributed to composition heterogeneity.

From the simultaneous dynamic and static LS measurements carried out at various angles, we can obtain information on the hydrodynamic radii and the radii of gyration of the particles. The diffusion coefficients were determined as slopes of the linear fit of the relaxation rates, Γ, versus $\sin^2(\theta/2)$ (Figure 8), and the corresponding hydrodynamic radii were calculated using the equation of Stokes−Einstein (eq 3). The radii of gyration, R_g, were obtained from the angular dependence of the quantity $1/(I \sin \theta)$ (Figure 10). Note that both R_h and R_g are not extrapolated to infinite dilution; i.e., they are radii at a certain concentration. Note also that R_g values are slightly overestimated since they are determined by using the total scattered light intensity, which contains a contribution from the unimers. For A2 and A3 that are discussed in the following, the latter is less than 2%. The combination of R_h and R_g yields the quantity R_g/R_h, which provides useful information about the particle density and structure.[45,46] The R_g/R_h value of A2 at 6 °C is 1.36, which is typical for starlike polymers or micelles.[46] For A3 at 5 °C a value of 0.75 was observed

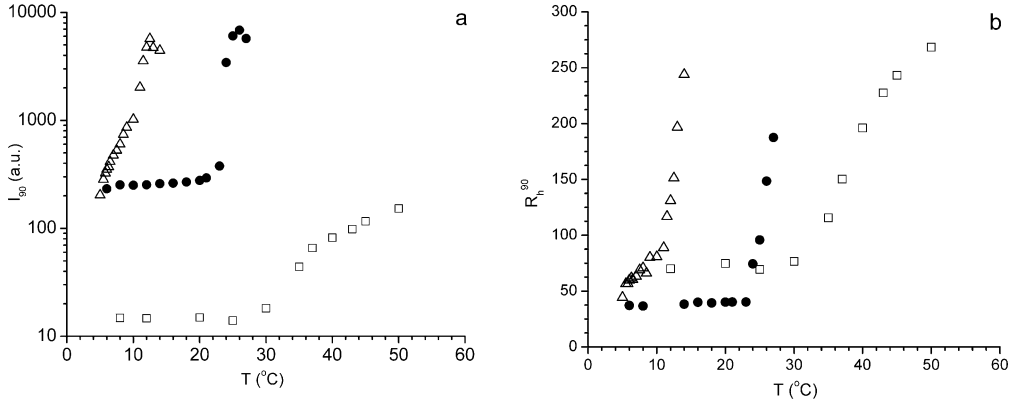

Figure 9. Variations of (a) light scattering intensity, I_{90}, and (b) hydrodynamic radii, R_h^{90}, measured at an angle of 90° of dispersions of A1 at 4.4 g/L (squares), A2 at 5.2 g/L (circles), and A3 at 3.2 g/L (triangles) as a function of temperature.

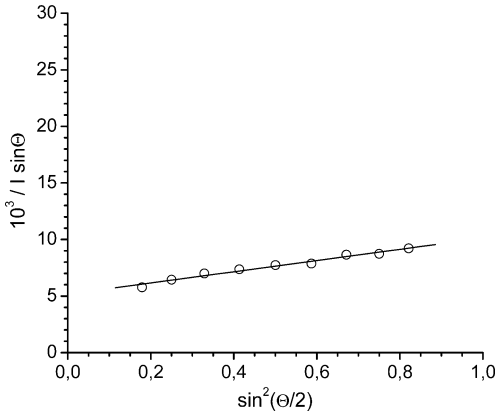

Figure 10. $1/(I \sin \theta)$ as a function of $\sin^2(\theta/2)$ for A2 at 5.2 g/L and 5 °C.

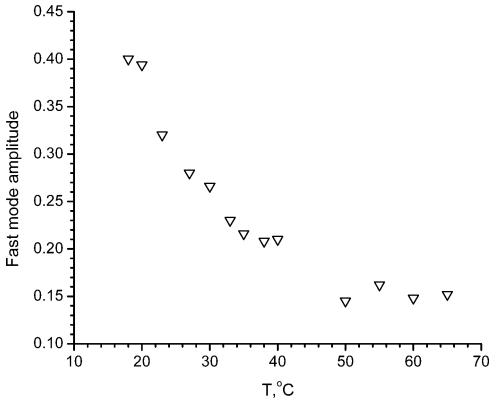

Figure 11. Variation of the amplitude of the fast mode of 5.7 g/L B1 as a function of temperature.

that is close to the value of 0.78 typifying hard spheres.[46] It is remarkable that the R_g/R_h values of the two copolymers are distinctly different although the temperatures at which they were determined were close. Obviously, the R_g/R_h values reflect formation of particles of different structures, which represent typical micelles for A2 and hard spheres for A3. A plausible explanation could be that the two copolymers are at different stages of aggregation. As discussed above, at 5 °C the secondary aggregation of the A3 particles must have already started. Interestingly and in full accordance with the interpretation we propose above, in the temperature region of the step increase of R_h^{90} and I_{90}, the R_g/R_h value of A2 was found to decrease and reach a value of 1.04 at 25 °C. This value is slightly higher than the expected one, which is about 0.78, which can be attributed to overestimation of the radius of gyration since at this particular temperature the relaxation time distribution function contains a low-amplitude slow mode, which affects R_g.

In general, the aggregation behavior of the PPO/PEEGE/PPO-type block copolymers is strongly composition and molecular weight dependent. As expected, the copolymers of low EEGE content are less able to self-associate than their counterparts of higher EEGE content. In the dilute region, however, invariably above the cmc's, a picture of isolated core/corona micellar particles can be derived from the data. The micelles presumably consist of PEEGE moieties gathered in the hydrophobic domains and PPO chains interacting with water. One can speculate on some penetration of PPO chains into the core since the particles are quite large to be spanned by the relatively short copolymer molecules. The micelles are stable and temperature-independent in a certain temperature interval. The width of these intervals is also composition-dependent. Presumably, for particular copolymer compositions (A3, for example) they are extremely short and exist only virtually. The high-temperature limit of these intervals is set by a secondary aggregation that is found to produce rather compact and dense particles.

3.2. PEEGE/PPO/PEEGE Architecture. The self-assembly tendency of copolymers with a reverse architecture is largely weakened as shown by a number of authors.[10,12,13] In line with these observations, the copolymers with a PEEGE/PPO/PEEGE sequence are water-soluble even at temperatures as high as 65 °C and clouding was not detected in the investigated concentration ranges. The relaxation time distributions of B1, B2, and B3 at concentrations higher than the cmc's contain invariably two diffusive modes (not shown). The fast modes are with substantially larger amplitudes compared to the corresponding amplitudes of the copolymers with a *normal* architecture. Their magnitudes are temperature-dependent and found to decrease with increasing temperature (Figure 11). As seen, the fast mode amplitude of B1 at 65 °C is about 15%, implying that there is a large fraction of unimers that are not incorporated in the aggregates even at that temperature. The fast modes correspond to particles with dimensions that are not dependent on the temperature. The radii are somewhat lower than those, calculated using eq 4. One can speculate that these are unimer molecules of lower than the average degrees of polymerization and/or cyclic molecules formed as a result of intramolecular hydrophobic interactions.[11,44]

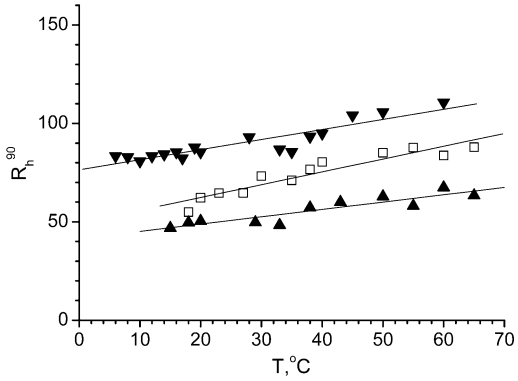

Figure 12. Variations of hydrodynamic radii, R_h^{90}, measured at an angle of 90° of dispersions of B1 at 5.7 g/L (squares), B3 at 8.2 g/L (inverted triangles), and B2 at 8.4 g/L (triangles) as a function of temperature. The lines through the data are drawn to guide the eye.

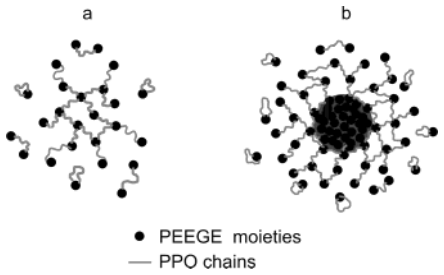

Figure 13. Schematic representation of possible states of chain association of PEEGE/PPO/PEEGE copolymers at low (a) and high (b) temperatures.

The dominant modes that are considered to reflect motions of aggregates are present in the whole temperature interval studied. The variations of the radii of the aggregates with temperature are shown in Figure 12. As can be seen the results scatter more compared to those of the copolymers with a PPO/PEEGE/PPO sequence, and composition dependencies can be hardly seen. This implies that the aggregation behavior is largely influenced by composition inhomogeneities. Nevertheless, one clear difference becomes quite obvious by comparing Figures 9b and 12: the dimensions of the aggregates are found to gradually increase with temperature in contrast to the sharp and sudden increase at a certain temperature, which is the case with the PPO/PEEGE/PPO copolymers. The difference can be explained by assuming different arrangements of the particles. Copolymers with a middle solvent-affinitive block are known to form branched or networklike structures due to interchain association of the terminal blocks.[11−13] It is conceivable to assume that physically cross-linked structures (Figure 13a) are formed at low temperatures by the EEGE-rich macromolecules. As the temperature increases they are easily converted into corelike structures due to the dehydration of the chains. At the same time, however, the changed environmental conditions induce a net transfer from unimers to aggregates. The unimers are of lower EEGE content and consequently more hydrophilic. They are presumably accommodated in the outer parts of the aggregates, thus forming coronae of branched or networklike structures that stabilize the hydrophobic cores (Figure 13b). Additionally, the hydrophobic junctions in the corona give rise to an effective increase of its thickness. The thicker corona provides better surface coverage, which could be a factor contributing to the stability of the particles by making them less sensitive to temperature-induced changes in the continuity and thickness of the corona.

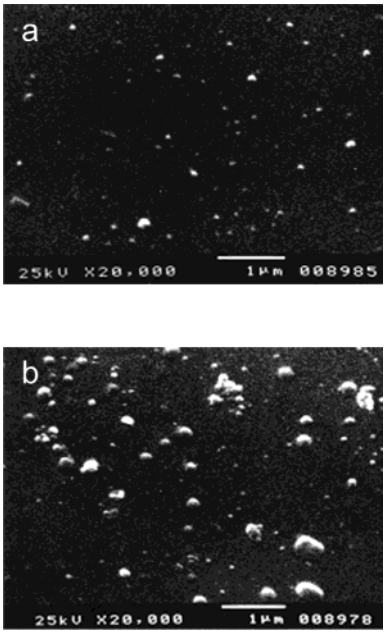

Figure 14. Particles prepared from sample B1: (a) 1% aqueous solution thermostated at 15 °C; (b) 1% aqueous solution thermostated at 20 °C.

The proposed model is not free of objections and has several questionable features. The most serious one is the length of the solvent-affinitive middle PPO block. It appears to be rather short, which would preclude the possibility of formation of associated structures. However, at the beginning of this section, we showed that a fraction of cyclic molecules formed as a result of intramolecular hydrophobic interactions involving looping of the middle block might exist. Furthermore, computer simulations on *small* symmetric triblock copolymers showed that branched and networklike assemblies might occur among the others.[47,48] On the basis of these findings, our model can be considered a feasible one. Moreover, it is consistent with and explains well the experimental data.

4. Scanning Electron Microscopy. Figure 14 shows micrographs of aggregates prepared from the copolymer B1 by the direct dissolution method. Before the preparation the solutions were thermostated at different temperatures. Two populations of particles can be distinguished in Figure 14a: particles of a radius of about 50 nm dominate the image; there is also a population of larger particles. At higher temperatures the shape and size of the particles become more diverse (Figure 14b). Small particles (ca. 50 nm in radius) coexist with large aggregates and clusters of size that reaches 1 μm.

D. Conclusions. Triblock copolymers of both ABA and BAB architectures of PO and EEGE were synthesized by means of anionic polymerization using cesium alkoxide initiating systems and characterized by SEC and NMR. The more hydrophobic block, PEEGE, was found to determine the LCST properties of the copolymers as well as their CP and cmc values. LS and SEM showed that the copolymers can form nanosized aggregates. Depending on the copolymer architecture, the latter exhibit different temperature behavior. Models describing different arrangements of the copolymer chains in the aggregates are proposed.

Acknowledgment. We acknowledge B. Trzebicka and I. Berlinova for helpful discussions.

References and Notes

(1) Wanka, G.; Hoffman, H.; Ulbricht, W. *Colloid Polym. Sci.* **1990**, *268*, 101.
(2) Mortensen, K.; Pedersen, J. *Macromolecules* **1993**, *26*, 805.
(3) Mortensen, K.; Brown, W. *Macromolecules* **1993**, *26*, 4128.
(4) Wanka, G.; Hoffman, H.; Ulbricht, W. *Macromolecules* **1994**, *27*, 4145.
(5) Alexandridis, P. *Curr. Opin. Colloid Interface Sci.* **1996**, *1*, 490.
(6) Michels, B.; Waton, G.; Zana, R. *Langmuir* **1997**, *13*, 3111.
(7) Kositza, M.; Bohne, C.; Alexandridis, P.; Hatton, T. A.; Holzwarth, J. F. *Macromolecules* **1999**, *32*, 5539.
(8) Chu, B. *Langmuir* **1995**, *11*, 414.
(9) Liu, T.; Zhou, Z.; Wu, C.; Chu, B.; Schneider, D.; Nace, V. *J. Phys. Chem. B* **1997**, *101*, 8808.
(10) Altinok, H.; Yu, G.; Nixon, S.; Gorry, P.; Attwood, D.; Booth, C. *Langmuir* **1997**, *13*, 5837.
(11) Alami, E.; Almgren, M.; Brown, W.; Francois, J. *Macromolecules* **1996**, *29*, 2229.
(12) Mortensen, K.; Brown, W.; Jorgensen, E. *Macromolecules* **1994**, *27*, 5654.
(13) Zhou, Z.; Chu, B. *Macromolecules* **1994**, *27*, 2025.
(14) Förster, S.; Antonietti, M. *Adv. Mater.* **1998**, *10*, 195.
(15) Allen, C.; Maysinger, D.; Eisenberg, A. *Colloids Surf., B* **1999**, *16*, 3.
(16) Torchilin, V. P. *J. Controlled Release* **2001**, *73*, 137.
(17) Jones, M.; Leroux, J. *Eur. J. Pharm. Biopharm.* **1999**, *48*, 101.
(18) Kwon, G.; Okano, T. *Adv. Drug Delivery Rev.* **1996**, *21*, 107.
(19) Riess, G. *Prog. Polym. Sci.* **2003**, *28*, 1107.
(20) Zhu, P.; Napper, D. *Langmuir* **2000**, *16*, 8543.
(21) Timoshenko, E.; Basovsky, R.; Kuznetsov, Y. *Colloids Surf., A* **2001**, *190*, 129.
(22) Robinson, K.; Paz-Banez, M.; Wang, X.; Armes, S. *Macromolecules* **2001**, *34*, 5799.
(23) Virtanen, J.; Holappa, S.; Lemmetyinen, H.; Tenhu, H. *Macromolecules* **2002**, *35*, 4763.
(24) Malmsten, M.; Linse, P.; Zhang, K.-W. *Macromolecules* **1993**, *26*, 2905.
(25) Mortensen, K.; Schwahn, D.; Janssen, S. *Phys. Rev. Lett.* **1993**, *71* (11), 1728.
(26) Schild, H. G.; Tirell, D. A. *J. Phys. Chem.* **1990**, *94*, 4352.
(27) Taton, D.; Le Borgne, A.; Sepulchre, M.; Spassky, N. *Macromol. Chem. Phys.* **1994**, *195*, 139.
(28) Dworak, A.; Baran, G.; Trzebicka, B.; Walach, W. *React. Funct. Polym.* **1999**, *42*, 31.
(29) Fitton, A.; Hill, J.; Jane, D.; Miller, R. *Synthesis* **1987**, 1140.
(30) Alexandridis, P.; Holzwarth, J. F.; Hatton, T. A. *Macromolecules* **1994**, *27*, 2414.
(31) Rangelov, S.; Brown, W. *Polymer* **2000**, *41*, 4825.
(32) Chu, B. *Laser Light Scattering*; Academic Press: New York, 1991; Vol. 2.
(33) Jakes, J. *Czech. J. Phys., B* **1988**, *38*, 1305.
(34) Simons, D. M.; Verbanc, J. J. *J. Polym. Sci.* **1960**, *XLIV*, 303.
(35) Ding, J.; Price, C. *Eur. Polym. J.* **1991**, *27*, 891.
(36) Ding, J.; Heatley, F.; Price, C.; Booth, C. *Eur. Polym. J.* **1991**, *27*, 895.
(37) Wegner, G.; Brandt, M.; Duda, L.; Hofmann, J.; Klesczewski, B.; Koch, D.; Kumpf, R.-J.; Orzesek, H.; Pirkl, H.-G.; Six, C.; Steinlein, C.; Weisbeck, M. *Appl. Catal., A* **2001**, *221*, 303.
(38) Rangelov, S.; Petrova, E.; Berlinova, I.; Tsvetanov, Ch. B. *Polymer* **2001**, *42*, 4483.
(39) Berlinova, I.; Dimitrov, I.; Kalinova, R.; Vladimirov, N. *Polymer* **2000**, *41*, 831.
(40) Dimitrov Ph.; Hasan. E.; Rangelov, S.; Trzebicka, B.; Dworak, A.; Tsvetanov, Ch. B. *Polymer* **2002**, *43*, 7171.
(41) Linse, P.; Malmsten, M. *Macromolecules* **1992**, *25*, 5434.
(42) Cotts, P. M.; Selser, J. C. *Macromolecules* **1990**, *23*, 2050.
(43) Stepanek, P. *J. Chem. Phys.* **1993**, *99*, 6384.
(44) Rangelov, S.; Almgren, M.; Tsvetanov, Ch.; Edwards, K. *Macromolecules* **2002**, *35*, 4770.
(45) Burchard, W. *Adv. Polym. Sci.* **1983**, *48*, 1.
(46) Thurn, A.; Burchard, W.; Niki, R. *Colloid Polym Sci.* **1987**, *265*, 653.
(47) Rodrigues, K.; Mattice, W. L. *Polym. Bull.* **1991**, *25*, 239.
(48) Rodrigues, K.; Mattice, W. L. *Langmuir* **1992**, *8*, 456.

MA0354039